

Electronic, Infrared, Raman, and Resonance Raman Spectroscopy of the Dirhodium Tetrakis(thiocarboxylate) Complexes $\text{Rh}_2(\text{OSCCH}_3)_4\text{L}_2$ ($\text{L} = \text{PPh}_3, \text{AsPh}_3, \text{SbPh}_3, \text{CH}_3\text{COSH}$)

Robin J. H. Clark,* David J. West, and Robert Withnall

Received July 24, 1991

The electronic, infrared, Raman, and resonance Raman spectra of the dirhodium tetrakis(thiocarboxylate) complexes $\text{Rh}_2(\text{C}-\text{H}_3\text{COS})_4\text{L}_2$ ($\text{L} = \text{PPh}_3, \text{AsPh}_3, \text{SbPh}_3, \text{CH}_3\text{COSH}$) have been recorded at temperatures down to 15 K. The $\sigma(\text{Rh}_2) \rightarrow \sigma^*(\text{Rh}_2)$ electronic transition occurs at 398–418 nm, some 2000–4000 cm^{-1} to lower wavenumber than for the analogous tetraacetate complexes. The wavenumber of the rhodium–rhodium stretching fundamental (226–251 cm^{-1}) is likewise some 60 cm^{-1} lower than that (289–307 cm^{-1}) found for the analogous tetraacetate complexes. Both spectroscopic results imply that the rhodium–rhodium bond in tetrakis(thioacetate) complexes is weaker than that in the analogous tetraacetate complexes, in keeping with the longer rhodium–rhodium bond lengths found crystallographically for the former.

Introduction

Raman and resonance Raman spectroscopy has previously been used to investigate the metal–metal bonding in the series of dirhodium tetraacetates, $\text{Rh}_2(\text{CH}_3\text{CO}_2)_4\text{L}_2$, dirhodium tetraacetamidates, $\text{Rh}_2(\text{CH}_3\text{CONH})_4\text{L}_2$, and dirhodium tetrakis(trifluoroacetamidate) complexes, $\text{Rh}_2(\text{CF}_3\text{CONH})_4\text{L}_2$ ($\text{L} = \text{PPh}_3, \text{AsPh}_3, \text{SbPh}_3$), and related complexes.^{1–7} It has been found that it is possible to distinguish between bands attributable to metal–metal and metal–bridge stretching fundamentals as the former are sensitive to the identity of the axial ligand, L, whereas to a first approximation the latter are not.

In this study, the four acetate bridging ligands have been replaced by the unsymmetrical ligands thioacetate. Only four X-ray crystal structures of dirhodium tetrakis(thiocarboxylate) complexes have so far been determined, and these demonstrate that the rhodium–rhodium bond length in such complexes, $r(\text{RhRh})$ (2.514–2.584 Å^{8–10}) is appreciably longer than that in analogous dirhodium tetracarboxylates. In the only previous Raman study of this class of compounds,¹¹ a single band was observed in the Raman spectra of $\text{Rh}_2(\text{CH}_3\text{COS})_4\cdot 2\text{CH}_3\text{CN}$ and $\text{Rh}_2(\text{CH}_3\text{COS})_4\cdot 2\text{C}_2\text{H}_5\text{N}$ at 154 and 164 cm^{-1} , respectively, and assigned to the rhodium–rhodium stretch in each case. These values for $\nu(\text{Rh}-\text{Rh})$ seem unreasonably low by comparison with values for $\nu(\text{Rh}-\text{Rh})$ of $\text{Rh}_2(\text{CH}_3\text{CO}_2)_4\cdot 2\text{L}$, $\text{Rh}_2(\text{CH}_3\text{CONH})_4\cdot 2\text{L}$, and $\text{Rh}_2(\text{CF}_3\text{CONH})_4\cdot 2\text{L}$ ($\text{L} = \text{PPh}_3, \text{AsPh}_3, \text{SbPh}_3$), which occur in the range 273.5–307 cm^{-1} .^{1–6} The present study was undertaken in order to characterize dirhodium tetrakis(thioacetate) complexes vibrationally and, in so doing, to establish the range of $\nu(\text{RhRh})$ values for several such complexes. The relationship between $\nu(\text{RhRh})$, $r(\text{RhRh})$, and the $\sigma(\text{RhRh}) \rightarrow \sigma^*(\text{RhRh})$ transition could then be set on a firm footing.

Experimental Section

Preparation of the Complexes. The complexes $\text{Rh}_2(\text{CH}_3\text{COS})_4\text{L}_2$ ($\text{L} = \text{PPh}_3, \text{AsPh}_3, \text{SbPh}_3$) were prepared in three steps. First, the di-

rhodium tetraformate complex, $\text{Rh}_2(\text{HCO}_2)_4\cdot 2\text{CH}_3\text{OH}$, was prepared from $\text{RhCl}_3\cdot 3\text{H}_2\text{O}$ by a literature method.¹² Second, the dirhodium tetraformate complex was stirred under nitrogen in a 10-fold excess of thioacetic acid at room temperature for 24 h yielding $\text{Rh}_2(\text{CH}_3\text{COS})_4\cdot 2\text{CH}_3\text{COSH}$. Finally, a methanolic solution of $\text{Rh}_2(\text{CH}_3\text{COS})_4\cdot 2\text{C}-\text{H}_3\text{COSH}$ was stirred under nitrogen with a saturated methanolic solution of the desired axial ligand. Each complex was recrystallized from dichloromethane. Anal. Calcd for $\text{Rh}_2(\text{CH}_3\text{COS})_4\cdot 2\text{PPh}_3$: C, 51.3; H, 4.11; S, 12.4; P, 6.01. Found: C, 51.4; H, 4.06; S, 12.4; P, 6.10. Calcd for $\text{Rh}_2(\text{CH}_3\text{COS})_4\cdot 2\text{AsPh}_3$: C, 47.2; H, 3.78; S, 11.5. Found: C, 46.5; H, 3.73; S, 11.3. Calcd for $\text{Rh}_2(\text{CH}_3\text{COS})_4\cdot 2\text{SbPh}_3$: C, 43.6; H, 3.49; S, 10.6. Found: C, 43.1; H, 3.44; S, 10.7. Calcd for $\text{Rh}_2(\text{CH}_3\text{COS})_4\cdot 2\text{CH}_3\text{COSH}$: C, 21.9; H, 3.04; S, 29.2. Found: C, 21.7; H, 3.01; S, 29.2.

Instrumentation. Raman spectra of the complexes were recorded with Spex 14018 (R6) and 1401 double grating monochromators, in conjunction with single photon counting detection using an RCA 31034A GaAs photomultiplier tube (with 647.1-nm excitation) and a Hamamatsu bialkali photomultiplier tube (with 406.7- or 457.9-nm excitation). The exciting radiation was provided by Coherent CR3000 K and CR18 lasers, and scattered light was collected with the 90° scattering geometry. Samples for Raman spectroscopy were pressed as undiluted disks and attached to the cold tip of an Air Products Displex closed-cycle helium refrigerator at ca. 15 K or a liquid nitrogen cooled cell at ca. 80 K. Disks for resonance Raman spectroscopy were diluted 90% with CsI. Infrared spectra were recorded on samples held at room temperature as CsI or wax disks at a spectral resolution of 1 cm^{-1} with a Bruker 113V FTIR spectrometer.

Solid-state transmission electronic spectra of the complexes in KBr disks and solution spectra of the complexes in dichloromethane solvent were recorded at room temperature on a Varian 2390 UV/vis spectrometer. Band maxima (nm) are as follows. $\text{Rh}_2(\text{CH}_3\text{COS})_4\cdot 2\text{PPh}_3$: solid 310 m, 415 s, ca. 475 w sh; solution 409 s, ca. 480 sh. $\text{Rh}_2(\text{CH}_3\text{COS})_4\cdot 2\text{AsPh}_3$: solid 310 m, 404 s, ca. 480 vw sh; solution 398 s, ca. 480 sh. $\text{Rh}_2(\text{CH}_3\text{COS})_4\cdot 2\text{SbPh}_3$: solid 310 m, 426 s, ca. 490 vw sh; solution 418 s, ca. 490 sh. The extinction coefficients of the strong band at ca. 400 nm are ca. 25 000 $\text{M}^{-1}\text{cm}^{-1}$. (s = strong, m = medium, w = weak, sh = shoulder, vw = very weak.)

Results and Discussion

Electronic Spectra. The transmission spectra of the complexes $\text{Rh}_2(\text{CH}_3\text{COS})_4\text{L}_2$ ($\text{L} = \text{PPh}_3, \text{AsPh}_3, \text{SbPh}_3$) in dichloromethane solution are shown over the visible region in Figure 1. Each solution contained a 100-fold excess of the axial ligand, L, in order to suppress dissociation of the complexes via the solution equilibrium, $\text{Rh}_2(\text{CH}_3\text{COS})_4\text{L}_2 \rightleftharpoons \text{Rh}_2(\text{CH}_3\text{COS})_4\text{L} + \text{L}$ ($\text{L} = \text{PPh}_3, \text{AsPh}_3, \text{SbPh}_3$). Under these conditions the electronic spectra were similar to those obtained for the complexes in the solid state as pressed KBr disks.

The band maxima occur in the blue region of the spectrum at 409, 398, and 418 nm for the complexes with $\text{L} = \text{PPh}_3, \text{AsPh}_3,$

- Clark, R. J. H.; Hempleman, A. J.; Flint, C. D. *J. Am. Chem. Soc.* **1986**, *108*, 518.
- Clark, R. J. H.; Hempleman, A. J. *Inorg. Chem.* **1988**, *27*, 2225.
- Clark, R. J. H.; Hempleman, A. J. *Inorg. Chem.* **1989**, *28*, 92.
- Clark, R. J. H.; Hempleman, A. J. *Inorg. Chem.* **1989**, *28*, 746.
- Best, S. P.; Chandley, P.; Clark, R. J. H.; McCarthy, S.; Hursthouse, M. B.; Bates, P. A. *J. Chem. Soc., Dalton Trans.* **1989**, 581.
- Best, S. P.; Clark, R. J. H.; Nightingale, A. J. *Inorg. Chem.* **1990**, *29*, 1383.
- Clark, R. J. H.; Hempleman, A. J. *Croat. Chem. Acta* **1988**, *61*, 313.
- Dikareva, L. M.; Porai-Koshits, M. A.; Sadikov, G. G.; Baranovskii, I. B.; Golubnichaya, M. A.; Shchelokov, R. N. *Russ. J. Inorg. Chem.* **1978**, *23*, 578.
- Morrison, E. C.; Tocher, D. A. *Inorg. Chim. Acta* **1989**, *156*, 99.
- Mehmet, N.; Tocher, D. A. *Inorg. Chim. Acta* **1991**, *188*, 71.
- Baranovskii, I. B.; Golubnichaya, M. A.; Mazo, G. Ya.; Nefedov, V. I.; Salyn', Ya. V.; Shchelokov, R. N. *Russ. Inorg. J. Chem.* **1976**, *21*, 591.

- Cotton, F. A.; Walton, R. A. *Multiple Bonds Between Metal Atoms*; Wiley: New York, 1982.

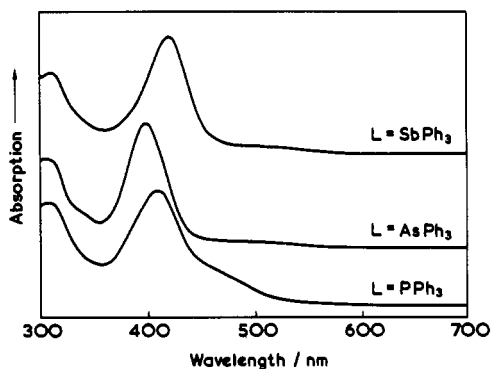


Figure 1. Electronic absorption spectra (700–300 nm) of dichloromethane solutions of Rh₂(CH₃COS)₄L₂ (L = PPh₃, AsPh₃, SbPh₃).

or SbPh₃, respectively, each in dichloromethane solution. The electronic spectrum of each complex also exhibits a weak shoulder at longer wavelength at ca. 480 nm with L = PPh₃ or AsPh₃ and at 490 nm with L = SbPh₃.

The strong band can be assigned to the allowed $\sigma(\text{Rh}_2) \rightarrow \sigma^*(\text{Rh}_2)$ transition, ${}^1B_u \leftarrow {}^1A_g$ in the C_{2h} point group, on intensity grounds. This transition is known to give rise to absorption bands with high extinction coefficients ($\epsilon > 10^4 \text{ M}^{-1} \text{ cm}^{-1}$) for analogous compounds such as the dirhodium tetraacetate compounds Rh₂(CH₃CO₂)₄(MPh₃)₂ with M = P, As, or Sb.^{1–4} Interestingly this absorption band has shifted to longer wavelength compared to its counterpart in the electronic spectra of the dirhodium tetraacetates for which it appears at 376, 352, and 361 nm with M = P, As, and Sb, respectively. This bathochromic shift of ca. 2000–4000 cm⁻¹ reflects the weakening of the $\sigma(\text{Rh}_2)$ bond in the thioacetate-bridged complexes compared to the acetate-bridged complexes. The weaker rhodium–rhodium bond is also manifested in a greater rhodium–rhodium bond length as made evident by the X-ray crystallographic data.^{8–10} The wavelength of the band maximum of the AsPh₃ adduct (398 nm) is shorter than those of the PPh₃ and SbPh₃ adducts (409 and 408 nm, respectively). The band maximum of the AsPh₃ adduct also occurs to shorter wavelength than that of the PPh₃ and SbPh₃ adducts in the electronic spectra of the acetates,³ acetamides,⁵ and trifluoroacetamides,⁶ although this ordering does not follow the trend in the basicities of these ligands viz. PPh₃ > AsPh₃ > SbPh₃. The reason possibly lies in the fact that the wavenumbers of the band maxima are sensitive to the extent of admixture of axial ligand lone-pair orbitals into the molecular orbitals forming the Rh–Rh bond. Indeed the energy of the orbital containing the lone-pair electrons for the phosphine ligands is known to come close to that of the LUMO of the Rh–Rh bond in dirhodium tetracarboxylates, resulting in significant mixing of the ligand and (Rh)₂ orbitals.¹²

Raman Spectra. The Raman spectra (647.1-nm excitation) of undiluted disks of Rh₂(CH₃COS)₄L₂ (L = PPh₃, AsPh₃, SbPh₃, CH₃COSH) are shown in Figures 2a–d over the important 200–350-cm⁻¹ region. The strong band occurring at 226, 239, 242, and 251 cm⁻¹ for the complexes with L = PPh₃, AsPh₃, SbPh₃, or CH₃COSH, respectively, can be confidently assigned to the rhodium–rhodium stretch, $\nu_1(\text{RhRh})$, on account of its wavenumber and its wavenumber dependence on the identity of the axial ligand, L. The band attributable to $\nu_1(\text{RhRh})$ in these complexes is expected to occur at an appreciably lower wavenumber than that (289–307 cm⁻¹) spanned by $\nu_1(\text{RhRh})$ of the tetraacetate complexes, Rh₂(CH₃CO₂)₄2L (L = PPh₃, AsPh₃, SbPh₃). The reason for this is that $\nu_1(\text{RhRh})$ is expected to bear a reciprocal relationship with the Rh–Rh bond distances and X-ray crystallographic studies provide evidence that the Rh–Rh bond distances in the tetrakis(thiocarboxylates) are considerably longer than in the tetraacetates, as will be discussed below. The trans influence of the axial ligand on the rhodium–rhodium bond follows the expected trend of bond weakening with increasing electron-donor ability along the series CH₃COSH < SbPh₃ < AsPh₃ < PPh₃; hence, $\nu_1(\text{RhRh})$ decreases along this series. This trans effect was similarly observed in previous studies of the analogous

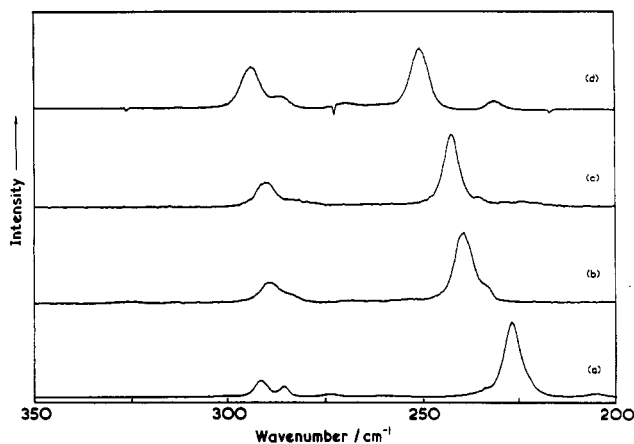


Figure 2. Raman spectra (350–200 cm⁻¹) of Rh₂(CH₃COS)₄L₂ as undiluted disks at ca. 80 K with 647.1-nm excitation with (a) L = PPh₃, (b) L = AsPh₃, (c) L = SbPh₃, and (d) L = CH₃COSH.

dirhodium tetraacetates² and is consistent with the X-ray structural data on Rh₂(CH₃COS)₄2CH₃COSH and Rh₂-((CH₃)₃CCOS)₄2PPh₃.^{8,9} The rhodium–rhodium distances in these compounds were reported to be 2.550 (3) and 2.584 (1) Å, respectively,^{8,9} which (as has previously been noted⁹) reflects the relative donor power of the axial triphenylphosphine and thioacetic acid ligands rather than any effect of changing the substituent on the bridging thiocarboxylate ligands (the replacement of a methyl substituent by a *tert*-butyl one is found for the dirhodium tetracarboxylates to lead to a shortening of the metal–metal bond^{12–14}). Indeed, a strong band at 239 cm⁻¹ in the Raman spectrum (647.1-nm excitation) of Rh₂((CH₃)₃CCOS)₄2PPh₃ is probably due to the rhodium–rhodium stretch of this complex, which suggests that its rhodium–rhodium bond length does come between that of Rh₂(CH₃COS)₄2PPh₃ and that of Rh(CH₃CO-S)₄2CH₃COSH.

It is interesting that $\nu_1(\text{RhRh})$ of Rh₂(CH₃COS)₄2PPh₃ occurs at 226 cm⁻¹, i.e. considerably lower than that (289 cm⁻¹)¹ of Rh₂(CH₃CO₂)₄2PPh₃. An empirical relationship between force constant (F) and bond length (r) has recently been used by Woodruff et al. to check the consistency of some assignments of rhodium–rhodium stretching modes in low-wavenumber Raman spectra of dirhodium compounds.¹⁵ The Rh–Rh bond length of 2.550 Å for Rh₂(CH₃COS)₄2CH₃COSH corresponds to a force constant of 1.84 mdyne/Å from the empirical relationship¹⁵ $r = 1.83 + 1.51[\exp(-F/2.48)]$. Taking this value of F , $\nu_1(\text{RhRh})$ of Rh₂(CH₃COS)₄2CH₃COSH should come at about 246 cm⁻¹ in good agreement with the experimentally determined value of 251 cm⁻¹. Similarly, the Rh–Rh bond length of 2.584 Å of Rh₂-((CH₃)₃CCOS)₄2PPh₃ corresponds to a force constant of 1.72 mdyne/Å, leading to an expected value for $\nu_1(\text{RhRh})$ of about 238 cm⁻¹ in very good agreement with the experimental value of 239 cm⁻¹.

The other prominent features in the spectra of Figure 2 are the bands at about 290 cm⁻¹, which are virtually insensitive to axial substitution. These bands are likely to arise from rhodium–bridge (either rhodium–oxygen or rhodium–sulfur) stretches.

The Raman ($\lambda = 647.1 \text{ nm}$) spectra of Rh₂(CH₃COS)₄2PPh₃ in the range 100–1600 cm⁻¹ are given in Figure 3. Similarly, Raman spectra of Rh₂(CH₃COS)₄2L (L = AsPh₃, SbPh₃, CH₃COSH) in the range 100–1600 cm⁻¹ were obtained and band listings together with their assignments are given in Tables I–IV. Whiffen's nomenclature¹⁶ has been used for assignments of bands due to the axial ligands.¹⁷

(13) Cotton, F. A.; Felthouse, T. R. *Inorg. Chem.* 1980, 19, 323.

(14) Cotton, F. A.; DeBoer, B. G.; LaPrade, M. D.; Pipal, J. R.; Ucko, D. A. *J. Am. Chem. Soc.* 1970, 92, 2926.

(15) Miskowski, V. M.; Dallinger, R. F.; Christoph, G. G.; Morris, D. E.; Spies, G. H.; Woodruff, W. H. *Inorg. Chem.* 1987, 26, 2127.

(16) Whiffen, D. H. *J. Chem. Soc.* 1956, 1350.

(17) Clark, R. J. H.; Flint, C. D.; Hempleman, A. J. *Spectrochim. Acta, Part A* 1987, 43A, 805.

Table I. Wavenumbers of Bands Observed in the Raman Spectrum^a of $\text{Rh}_2(\text{CH}_3\text{COS})_4\cdot 2\text{PPh}_3$ at ca. 15 K

$\bar{\nu}/\text{cm}^{-1}$	assgnt	$\bar{\nu}/\text{cm}^{-1}$	assgnt ^b
93 w		619 vw	$\alpha(\text{C}-\text{C}-\text{C})$
100 w		670 vw	
204 w	$\delta(\text{ring})$	686 vw	r X-sens
226 vs	$\nu(\text{Rh}-\text{Rh})$	704 w	$\nu(\text{C}-\text{S})$
272 w		743 vw	
285 w		751 vw	
291 m	$\nu(\text{Rh}-\text{bridge})$	757 vw	$\gamma(\text{C}-\text{H})$
389 w		851 vw	
392 w	w $\rho(\text{C}-\text{C})$	884 vw	$\gamma(\text{C}-\text{H})$
402 w		932 vw	$\gamma(\text{C}-\text{H})$
416 w		1000 m	p-ring
439 w		1031 w	$\beta(\text{C}-\text{H})$
451 w		1096 m	q X-sens
493 w		1159 vw	$\beta(\text{C}-\text{H})$
497 w		1188 vw	$\beta(\text{C}-\text{H})$
502 w		1432 vw	$\nu(\text{C}-\text{C})$
520 m	y X-sens	1484 vw	$\nu(\text{C}-\text{C})$
582 w		1587 m	$\nu(\text{C}-\text{C})$

^a 647.1-nm excitation. ^b Whiffen's notation.¹⁶**Table II.** Wavenumbers of Bands Observed in the Raman Spectrum^a of $\text{Rh}_2(\text{CH}_3\text{COS})_4\cdot 2\text{AsPh}_3$ at ca. 80 K

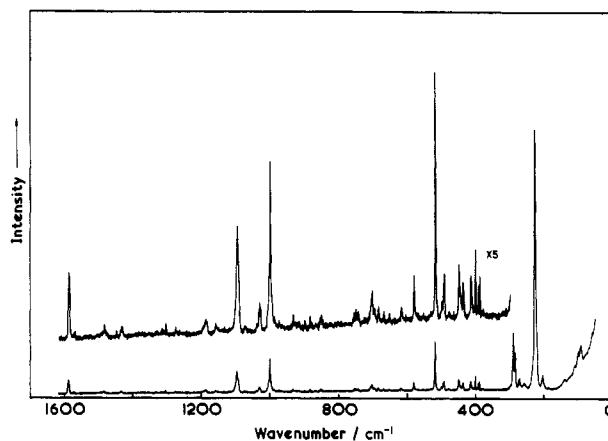
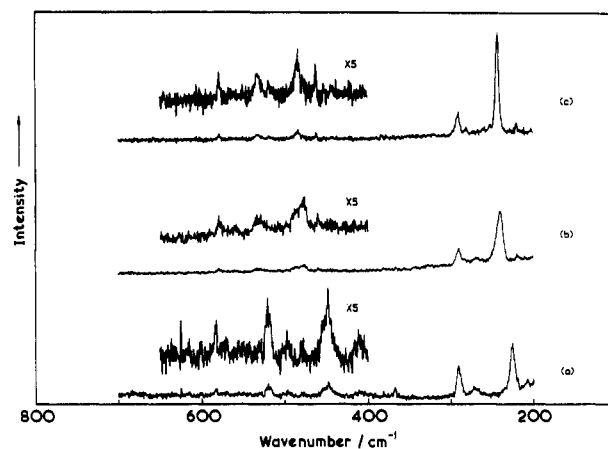
$\bar{\nu}/\text{cm}^{-1}$	assgnt	$\bar{\nu}/\text{cm}^{-1}$	assgnt ^b
187 w	x X-sens	686 vw	
239 s	$\nu(\text{Rh}-\text{Rh})$	696 vw	$\rho(\text{C}-\text{C})$
252 vw		1002 m	p-ring
267 vw		1027 vw	$\beta(\text{C}-\text{H})$
289 m	$\nu(\text{Rh}-\text{bridge})$	1079 vw	q X-sens
324 vw	$\nu(\text{Rh}-\text{bridge})$	1086 vw	q X-sens
443 vw		1155 vw	$\beta(\text{C}-\text{H})$
467 vw		1190 vw	$\beta(\text{C}-\text{H})$
473 vw		1310 vw	
478 vw		1319 vw	
581 vw		1435 vw	
600 vw		1574 vw	$\nu(\text{C}-\text{C})$
617 vw	$\alpha(\text{C}-\text{C}-\text{C})$	1584 w	$\nu(\text{C}-\text{C})$
670 w	r X-sens		

^a 647.1-nm excitation. ^b Whiffen's notation.¹⁶**Table III.** Wavenumbers of Bands Observed in the Raman Spectrum^a of $\text{Rh}_2(\text{CH}_3\text{COS})_4\cdot 2\text{SbPh}_3$ at ca. 80 K

$\bar{\nu}/\text{cm}^{-1}$	assgnt	$\bar{\nu}/\text{cm}^{-1}$	assgnt ^b
164 vw	x X-sens	699 vw	v $\rho(\text{C}-\text{C})$
175 vw	x X-sens	1002 m	p-ring
223 vw	u X-sens	1025 vw	$\beta(\text{C}-\text{H})$
242 s	$\nu(\text{Rh}-\text{Rh})$	1074 vw	q X-sens
289 m	$\nu(\text{Rh}-\text{bridge})$	1335 vw	
449 vw		1433 vw	n $\nu(\text{C}-\text{C})$
456 vw	y X-sens	1452 vw	
578 w		1582 vw	$\nu(\text{C}-\text{C})$
659 m	r X-sens	1594 vw	$\nu(\text{C}-\text{C})$

^a 647.1-nm excitation. ^b Whiffen's notation.¹⁶**Table IV.** Wavenumbers of Bands Observed in the Raman Spectrum^a of $\text{Rh}_2(\text{CH}_3\text{COS})_4\cdot 2\text{CH}_3\text{COSH}$ at ca. 80 K

$\bar{\nu}/\text{cm}^{-1}$	assgnt	$\bar{\nu}/\text{cm}^{-1}$	assgnt
132 m		527 w	
161 m		572 w	
232 w	$\delta(\text{ring})$	613 w	
251 s	$\nu(\text{Rh}-\text{Rh})$	724 m	$\nu(\text{C}-\text{S})$
270 w		1003 w	
287 w		1152 w	
294 s	$\nu(\text{Rh}-\text{bridge})$	1320 w	
394 w		1353 w	$\delta(\text{CH}_3)$
451 w		1368 w	
503 w		1416 w	

^a 647.1-nm excitation.**Resonance Raman Spectra.** The resonance Raman spectra of $\text{Rh}_2(\text{CH}_3\text{COS})_4\cdot 2\text{L}$ (L = PPh_3 , AsPh_3 , SbPh_3) are shown in Figure**Figure 3.** Raman spectrum (1600–100 cm^{-1}) of $\text{Rh}_2(\text{CH}_3\text{COS})_4\cdot 2\text{PPh}_3$ as an undiluted disk at ca. 15 K with 647.1-nm excitation.**Figure 4.** Resonance Raman spectra (700–200 cm^{-1}) of $\text{Rh}_2(\text{CH}_3\text{COS})_4\cdot 2\text{L}$ as KCl disks at ca. 15 K with (a) L = PPh_3 and 457.9-nm excitation, (b) L = AsPh_3 and 406.7-nm excitation, and (c) L = SbPh_3 and 406.7-nm excitation.**Table V.** Wavenumbers (cm^{-1}) of Bands Observed in the Resonance Raman Spectrum of $\text{Rh}_2(\text{CH}_3\text{COS})_4\cdot 2\text{L}$ (L = PPh_3 , AsPh_3 , SbPh_3) Complexes

assgnt	PPh_3^a	AsPh_3^b	SbPh_3^b
$\nu_1(\text{Rh}-\text{Rh})$	226	239	242
$\nu_2(\text{Rh}-\text{bridge})$	291	290	290
$2\nu_1$	447	478	483
$\nu_1 + \nu_2$	518	532	532
$2\nu_2$	581	580	579

^a 457.9-nm excitation. ^b 406.7-nm excitation.**Table VI.** Wavenumbers of Bands Observed in the Far-Infrared (600–200 cm^{-1}) Spectra of the Complexes $\text{Rh}_2(\text{CH}_3\text{COS})_4\cdot 2\text{L}$ (L = PPh_3 , AsPh_3 , SbPh_3) at 298 K^a

PPh_3		AsPh_3		SbPh_3	
$\bar{\nu}/\text{cm}^{-1}$	assgnt	$\bar{\nu}/\text{cm}^{-1}$	assgnt	$\bar{\nu}/\text{cm}^{-1}$	assgnt
555 m	$\delta(\text{OCS})$	551 m	$\delta(\text{OCS})$	549 m	$\delta(\text{OCS})$
514 s	y X-sens	472 s	y X-sens	450 s	y X-sens
502 s	y X-sens	441 w	w $\phi(\text{C}-\text{C})$	316 m	$\nu(\text{Rh}-\text{O})$
496 s	y X-sens	319 s	$\nu(\text{Rh}-\text{O})$, t X-sens	279 w	$\nu(\text{Rh}-\text{S})$
446 m	t X-sens	279 w	$\nu(\text{Rh}-\text{S})$	265 s	t X-sens
410 m	r, u or w				
396 w	w $\phi(\text{C}-\text{C})$				
316 m	$\nu(\text{Rh}-\text{O})$				
280 w	$\nu(\text{Rh}-\text{S})$				
255 w	u X-sens				
220 w	x X-sens				

^a Whiffen's notation.¹⁶4. They exhibit an overtone and combination tone of $\nu_1(\text{RhRh})$ and $\nu_2(\text{Rh-bridge})$, the wavenumbers of which are listed in Table

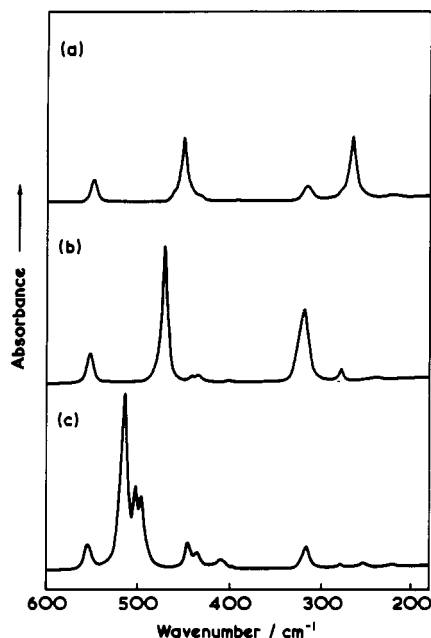


Figure 5. Far-infrared spectra (600–200 cm^{-1}) of $\text{Rh}_2(\text{CH}_3\text{COS})_4\text{L}_2$ as wax disks at room temperature with (a) $\text{L} = \text{PPh}_3$, (b) $\text{L} = \text{AsPh}_3$, and (c) $\text{L} = \text{SbPh}_3$.

V. The appearance of an overtone and combination tone involving $\nu_1(\text{RhRh})$ in the Raman spectra taken at resonance with the ca. 400-nm band supports the earlier assignment of this electronic transition to $\sigma(\text{RhRh}) \rightarrow \sigma^*(\text{RhRh})$, since the Rh–Rh bond length in the σ^* state would be expected to be longer than in the ground state. However, the appearance of an overtone of $\nu_2(\text{Rh-bridge})$ suggests that the resonant transition may have some Rh–bridge character to it as well. Moreover, the lack of long progressions in ν_1 at resonance with the $\sigma \rightarrow \sigma^*$ transition (such as are typical of the resonance Raman spectra of the analogous tetraacetate complexes) indicates that excitation leads to small geometric changes along several coordinates rather than to a more substantial

change essentially along the ν_1 coordinate alone.¹⁹

Infrared Spectra. Far-infrared spectra of $\text{Rh}_2(\text{CH}_3\text{COS})_4\cdot 2\text{L}$ ($\text{L} = \text{PPh}_3, \text{AsPh}_3, \text{SbPh}_3$) are shown in Figure 5, and the bands have been listed in Table VI along with their assignments. Three bands at 279, 316, and 550 cm^{-1} in each spectrum shift very little on changing L, and these have been assigned to infrared-active $\nu(\text{Rh-S}), \nu(\text{Rh-O}),$ and $\delta(\text{OCS})$ modes of the $\text{Rh}_2(\text{CH}_3\text{COS})_4$ skeleton by comparison with assignments for analogous compounds.^{11,18} Strong bands at 496, 502, and 514 cm^{-1} , with $\text{L} = \text{PPh}_3$, do show a dependence on axial ligand, shifting to 472 cm^{-1} with $\text{L} = \text{AsPh}_3$ and 450 cm^{-1} with $\text{L} = \text{SbPh}_3$. These are assigned to $\gamma\text{-X-sens}$ and $t\text{-X-sens}$ modes (Whiffen's nomenclature^{16,17}) of the axial ligands by analogy with previous assignments of bands observed at similar wavenumbers in the spectra of $\text{Rh}_2(\text{CH}_3\text{CO}_2)_4\cdot 2\text{L}$ ($\text{L} = \text{PPh}_3, \text{AsPh}_3, \text{SbPh}_3$).¹⁻³

Intense bands attributable to skeletal $\nu(\text{C-S})$ and $\nu(\text{C-O})$ modes appear at 703 and 1545 cm^{-1} with $\text{L} = \text{PPh}_3$, 697 and 1548 cm^{-1} with $\text{L} = \text{AsPh}_3$, and 698 and 1544 cm^{-1} with $\text{L} = \text{SbPh}_3$. These have been assigned by comparison with literature infrared spectra of analogous compounds.¹⁸

Conclusion

The electronic and resonance Raman spectra of the complexes studied are fully consistent with the evidence from X-ray crystallographic studies that the Rh–Rh bond distance in dirhodium tetrakis(thiocarboxylates) is considerably longer than in dirhodium tetracarboxylates. The strong band in the blue region of the visible spectrum of the tetrakis(thioacetates) is assigned to the $\sigma(\text{Rh})_2 \rightarrow \sigma^*(\text{Rh})_2$ transition; it exhibits a bathochromic shift of ca. 2000–4000 cm^{-1} relative to that found for the analogous dirhodium tetraacetate, this being indicative of a weaker, longer $\sigma(\text{Rh})_2$ bond for the former. The most intense band in the Raman and resonance Raman spectra of $\text{Rh}_2(\text{CH}_3\text{COS})_4\cdot 2\text{L}$ ($\text{L} = \text{PPh}_3, \text{AsPh}_3, \text{SbPh}_3$) is assigned to $\nu_1(\text{RhRh})$ at 226–242 cm^{-1} . It occurs at an appreciably lower wavenumber than $\nu_1(\text{RhRh})$ of $\text{Rh}_2(\text{CH}_3\text{CO}_2)_4\cdot 2\text{L}$ ($\text{L} = \text{PPh}_3, \text{AsPh}_3, \text{SbPh}_3$) (289–307 cm^{-1}), and this is also in keeping with a weaker, longer Rh–Rh bond in tetrakis(thioacetates) than in tetraacetates.

Acknowledgment. We are grateful to the Wolfson Foundation for a grant (to support R.W.) and to the ULIRS for support.

(18) Kireeva, I. K.; Mazo, G. Ya.; Shchelokov, R. N. *Russian Inorg. J. Chem.* 1979, 24, 220.

(19) Clark, R. J. H.; Dines, T. J. *Angew. Chem., Int. Ed. Engl.* 1986, 25, 131.

Contribution from the Departments of Chemistry, College of General Education, Nagoya University, Chikusa-ku, Nagoya 464-01, Japan, College of General Education, Osaka University, Toyonaka, 560 Japan, and Daido Institute of Technology, Minami-ku, Nagoya, 457 Japan

XANES Spectra of Copper(II) Complexes: Correlation of the Intensity of the $1s \rightarrow 3d$ Transition and the Shape of the Complex

Mitsuru Sano,^{*,†} Seiko Komorita,[‡] and Hideo Yamatera[§]

Received July 6, 1990

X-ray absorption spectra are measured for several copper complexes with four identical ligands, $[\text{CuL}_4]^{2-}$ ($\text{L} = \text{chloro, succinimidato}$), whose geometry ranges from tetrahedral to square planar. Although the main features change complicatedly, the intensity of the $1s \rightarrow 3d$ peak increases with the increase in the dihedral angle between the two L-Cu-L planes. The relation between the intensity and the dihedral angle is explained by correlating the intensity with the mixing of the Cu 3d and 4p orbitals through the perturbation of the ligand field.

Introduction

XANES gives information complementary to that extracted from EXAFS concerning the coordination geometry and electronic structure an absorbing atom; this is particularly important in the

study of systems for which EXAFS is of limited usefulness.¹ Although X-ray absorption spectra near K-edge have been reported for many years, the relations between the spectral characteristics such as the intensity, shape, and location of edge features and the ligand field geometry and electronic structure of the absorbing atom still remain to be addressed in further systematic

[†]Nagoya University.

[‡]Osaka University.

[§]Daido Institute of Technology.

(1) Bianconi, A.; Garofalo, J.; Benfatto, M. *Top. Current Chem.* 1988, 145, 29.